Theory and Experiments on Elastic Band Gaps

D. García-Pablos,[1] M. Sigalas,[1,2] F. R. Montero de Espinosa,[3] M. Torres,[4] M. Kafesaki,[1] and N. García[1]

[1]*Laboratorio de Fisica de Sistemas Pequeños y Nanotecnología, Consejo Superior de Investigaciones Científicas (CSIC), Serrano 144, 28006 Madrid, Spain*

[2]*Ames Laboratory, Iowa State University, Ames, Iowa 50011*

[3]*Instituto de Acústica, CSIC, Serrano 144, 28006 Madrid, Spain*

[4]*Instituto de Física Aplicada, CSIC, Serrano 144, 28006 Madrid, Spain*

(Received 26 February 1999)

We study elastic band gaps in nonhomogeneous periodic finite media. The finite-difference time-domain method is used for the first time in the field of elastic band-gap materials. It is used to interpret experimental data for two-dimensional systems consisting of cylinders of fluids (Hg, air, and oil) inserted periodically in a finite slab of aluminum host. The method provides good convergence, can be applied to realistic finite composite slabs, even to composites with a huge contrast in the elastic parameters of their components, and describes well the experiments.

PACS numbers: 43.20.+g, 43.35.+d, 43.40.+s

The study of propagation of waves in inhomogeneous media is a problem of wide interest because of the implications in technology and the broad view that can be supplied in understanding a large area of physical problems. Band structure of electrons in solids [1] has been amply studied for many years. Many of their properties have been also mimicked in what is known as photonic band-gap materials [2–5]. Early work [6–8] also explored the propagation of sound and full elastic waves (ELW) by calculating the band structure of infinite periodic systems with Fourier transform of the wave equation. Other frequency domain treatments have been also applied [9]. Experiments on band gaps [10], surface states, wave guides, and localization in defects [11] of elastic media have proved the ample and versatile possibilities of the elastic systems because the typical sizes of the inhomogeneities we are referring to (periodicity in the case of "crystalline" systems) are millimeters. This is very important because it is possible to generate all kind of complicated structures by just drilling holes.

Up to now the plane wave (PW) method has been used for the calculation of elastic band gaps. However, this approach presents convergence problems for the full elastic wave equation when liquids are inserted in a solid host [8]. The reason for the convergence problems is related to the zero transverse velocity (as well as μ Lamé coefficient) in the liquid. For that reason the finite Fourier transform of the μ does not converge. A way to solve this problem is to use an imaginary μ, thereby accounting for fluid viscosity. We have estimated, however, that the ratios of the imaginary parts of μ of the components in the composites studied are very large (around 10^6) and therefore the problem may remain, although it should be given further consideration. Besides, the PW method calculates the band structure of ELW propagating in infinitely long periodic systems and its results can be only indirectly compared with transmission measurements in a finite system. In addition, the PW does not take into account the reflectivity of the waves at the interface between the periodic medium and the surrounding homogeneous environment, a phenomenon that exists for finite samples. A different approach is then needed. In order to solve these problems we have developed a code for the temporal integration of incident wave packets for the full elastic equation. The motivation for a finite difference time domain (FDTD) method [12] is clear: It does not present the above mentioned convergence problems (reliability of FDTD schemes depends on discretization, and our calculations show no convergence problem for small enough time and space steps satisfying the necessary stability criteria). It allows us to study finite systems and to simulate the experiments in the same way that they are carried out. It provides at any time the displacement field at every point. The FDTD results presented here are compared with experiments on two-dimensional (2D) systems where Al is used as a host medium and the inserted fluids are Hg, oil, and air. This type of sample was previously investigated in Refs. [10,11]. We proceed first by describing the method of calculation.

The elastic wave equation in inhomogeneous solids is given by

$$\frac{\partial^2 u^i}{\partial t^2} = \frac{1}{\rho}\left\{\frac{\partial}{\partial x_i}\left(\lambda \frac{\partial u^l}{\partial x_l}\right) + \frac{\partial}{\partial x_l}\left[\mu\left(\frac{\partial u^i}{\partial x_l} + \frac{\partial u^l}{\partial x_i}\right)\right]\right\}, \tag{1}$$

where u^i is the ith component of the displacement vector $\mathbf{u}(\mathbf{r})$, $\lambda(\mathbf{r})$ and $\mu(\mathbf{r})$ are the Lamé coefficients [13], and $\rho(\mathbf{r})$ is the mass density. We study propagation in a composite medium consisting of identical parallel and infinitely long cylinders embedded within a square periodic

array in a host material. The system has translational symmetry along the axis of the cylinders (z), thus the material parameters do not depend on the coordinate z. By assuming propagation in the x-y (perpendicular to the cylinders axes) plane, the wave equation can split into two independent equations [6,7], one for the z component of the field (u_z), and one for the x and y components (u_x and u_y, respectively). The second one involves both longitudinal and transverse waves and this is the equation which we study here:

$$\rho \frac{\partial^2 u_x}{\partial t^2} = \frac{\partial T_{xx}}{\partial x} + \frac{\partial T_{xy}}{\partial y}, \qquad \rho \frac{\partial^2 u_y}{\partial t^2} = \frac{\partial T_{xy}}{\partial x} + \frac{\partial T_{yy}}{\partial y}. \tag{2}$$

$T_{xx} = (\lambda + 2\mu)\partial u_x/\partial x + \lambda \partial u_y/\partial y$, $T_{yy} = (\lambda + 2\mu)\partial u_y/\partial y + \lambda \partial u_x/\partial x$, and $T_{xy} = \mu(\partial u_x/\partial y + \partial u_y/\partial x)$. The longitudinal velocity c_l and the transverse one c_t are given by $c_l = \sqrt{(\lambda + 2\mu)/\rho}$ and $c_t = \sqrt{\mu/\rho}$.

In this work the wave equations (2) are integrated by means of a FDTD [12,14] scheme which uses discretization of the equations in both the space and the time domains. It sets appropriate boundary conditions, and explicitly calculates the evolution of **u** in the time domain. More specifically, real space is discretized into a rectangular grid where all the variables are defined; u_x and u_y are spatially interlaced by half a grid cell; the elastic wave equations are approximated by center differences in both space and time. The computational cell contains a slab of the composite medium in its central part. The slab is finite along the y direction containing N_y cylinders (see the inset in Fig. 1). Mur's first order absorbing boundary conditions [12,15] are used at the boundaries of the computational cell along the x axis. At the boundaries along the y axis, periodic boundary conditions are used. This is a good approximation of the experimentally studied structure which consists of 15 cylinders along the x axis. Plane wave packets containing a wide range of frequencies are launched from the negative y direction and they are normally incident on the surface of the composite. The displacement vectors u_x and u_y are collected as a function of time at a detection point in the other side of the composite. By using fast Fourier transform and by normalizing with the incident wave frequency profile, we can find the transmission coefficient, and thus the attenuation, as a function of frequency. In order to cover a wide range of frequencies (from 0.3 up to 1.5 MHz) four Gaussian pulses are launched, covering different frequency regimes. It is remarkable the perfect overlapping of different calculations for common frequency regions. This fact demonstrates the consistency of our approach.

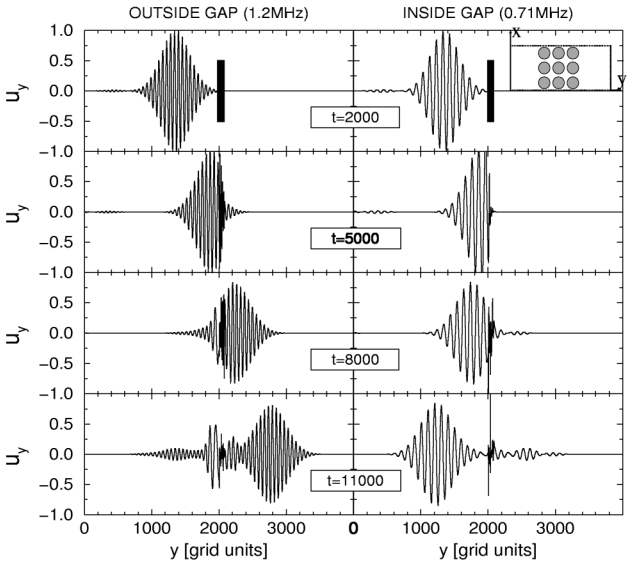

FIG. 1. Longitudinal field component, $u_y(x, y, t)$, as a function of y at four different times for two narrow Gaussian wave packets centered at a frequency out of any band gap (left-side plots) and inside a frequency band gap (right-side plots). System parameters: Hg in Al, $f = 0.42$, $a = 2.73$ mm. The black rectangles represent the slab containing the cylinders, which is shown more clearly in the small figure inset in the upper right panel. Time is given in time step units ($\tau_0 = 2.53 \times 10^{-9}$ s).

The filling fraction f of the cylinders in a square lattice is given by $f = \pi r^2/a^2$ where r is the radius of the cylinders and a is the lattice constant. The relevant parameters for the simulations are the grid spacings dx and dy, the time step dt, the number of cylinders in the y direction (N_y), and the amount of time steps which sets the frequency resolution. Most of the calculations shown here correspond to $dx = dy = a/30$, $dt = 5.89 \times 10^{-3} a/c_l^{Al}$, and $N_y = 3$. The cylinder radius is kept constant (1 mm), and a varies in order to change the filling ratio. Satisfactory convergence tests have been carried out, calculating the propagation for different grid spacings and a different number of cylinders. (For more details on the application of the FDTD in 2D elastic binary composites, see Ref. [14].)

Regarding the experimental measurements, samples consisting of aluminum parallelepipeds of $50 \times 40 \times 15$ mm^3 (Alplan MEC 7079 T 651) were carefully drilled all along their thickness according to a square arrangement. Mercury, baby oil ($\rho = 0.82$ g/cm^3), and air were used to fill the cylindrical holes ($r = 1$ mm) of the samples. Care was taken when filling the samples in order to avoid the appearance of air bubbles between the liquid and the aluminum walls. Standard vacuum techniques were used. The acoustic attenuation of the samples (reduction in power transmission) was measured using the gain-phase module of a HP 4194 A impedance gain-phase analyzer. Samples were sandwiched between the transducers, including two delay lines between each transducer and the block surface in a pitch-catch arrangement. The wave front impinging the blocks is just in the near-far field transition where the front can be considered plane. In all cases pure aluminum blocks with the same geometry were measured in order to separate the true

attenuation due to the band structure and the intrinsic losses. With this technique, the structural attenuation as a function of frequency was directly obtained.

Figure 1 shows a representative FDTD result for the ELW propagation in a band-gap material. The system consists of Hg cylinders in an Al host. Left-hand side curves correspond to the longitudinal component of **u** as a function of space at four different times for a narrow incident wave packet of frequencies out of any band gap. Right-hand side curves correspond to a pulse inside the frequency band gap. Following the sequence in time, we can see how the pulse outside the gap crosses the slab (situated in the middle of the computational cell—see black rectangle in the top panels) without big reflections (although not with zero reflectivity due to impedance mismatch between homogeneous host and periodic slab). On the other hand, the pulse inside the gap is almost fully reflected when it reaches the slab.

Figure 2 presents the transmission coefficients for a system of Hg cylinders inserted in Al, for four different Hg filling ratios. Figure 2(d) corresponds to the sample studied in Fig. 1 and shows two clear gaps: 0.55–0.75 MHz and 0.87–1.05 MHz, approximately. The filling ratio dependence studied in Fig. 2 shows how the gap width does not change much for this system. However, as the filling ratio increases we can notice how the gap gets wider and how a peak of transmitted amplitude emerges in the middle, separating two distinct gaps.

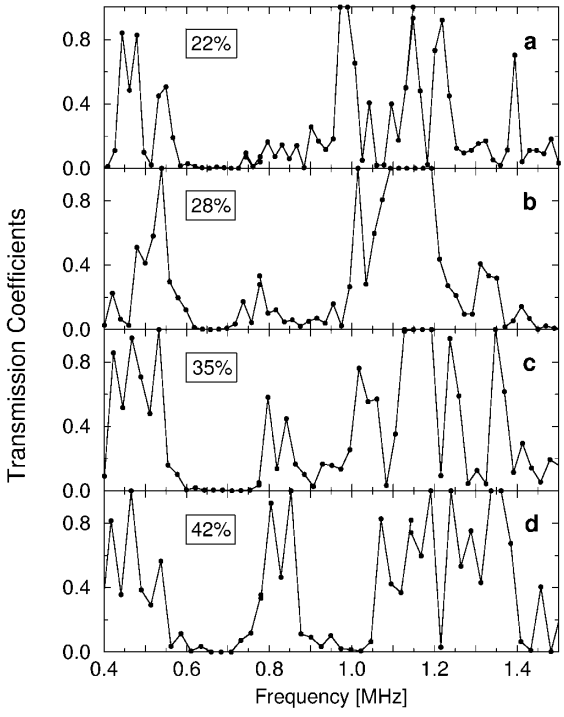

FIG. 2. Transmission coefficient vs frequency for four filling ratios (f) of Hg cylinders in Al host: (a) $f = 0.22$, (b) $f = 0.28$, (c) $f = 0.35$, and (d) $f = 0.42$. In all cases $r = 1$ mm.

We have carried out extensive calculations for different materials, different filling ratios, and for both the ⟨100⟩ and the ⟨110⟩ direction, as well as the corresponding experiments. Next we present some representative theoretical and experimental results showing the existence and the size of significant frequency stop bands for the materials studied and illustrating the validity of the FDTD method in the investigation of the elastic wave propagation in inhomogeneous media.

Samples with Hg cylinders are studied also in Fig. 3. Attenuation deeps are found experimentally along the ⟨100⟩ direction for a sample with 42% filling of Hg [see Fig. 3(a), solid line] at around (~) 0.75 and 1.0 MHz, with a 20 dB humplike region (peak) between them. The FDTD calculation [Fig. 3(a), dashed line] leads to a strongly attenuated frequency region at ~0.75–1.0 MHz, with the above mentioned peak of transmitted amplitude centered at ~0.8 MHz. The peak, which is due to a flat band appearance at this filling ratio, is also found for 40% filling (not shown here), although smaller, reproducing the trend observed in Fig. 2. The agreement between theory and experiments is good taking into account the intrinsic difficulties of the measurements, the FDTD method error sources, and other factors not considered, such as friction. Figure 3(b) provides the comparison between the experimental and the numerical attenuation for $f = 0.4$ along the ⟨110⟩ direction. The experimental attenuation dip at ~0.55–0.85 MHz is in excellent agreement with the FDTD result. The experiments and calculations discussed in connection with this figure prove the existence of band gaps for the 40% Hg filling sample at the ⟨100⟩ and ⟨110⟩ directions. Probably it is going for a full band gap. However, experiments in other directions are more complicated because of geometry and cutting of the samples.

In Fig. 4 we show results for samples filled with oil and air. Figure 4(a) shows the attenuation vs frequency for a

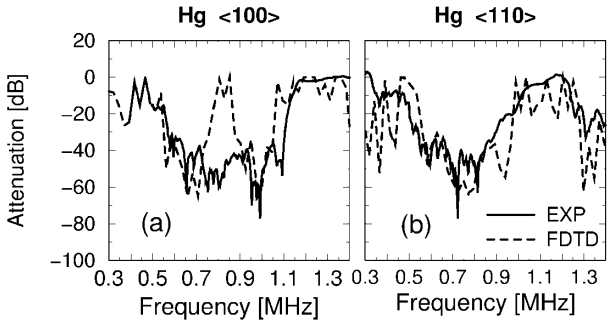

FIG. 3. Experimental (solid lines) and calculated (dashed lines) attenuation vs frequency for two samples of Al with cylinders filled up with Hg. (a) $f = 0.42$, along the ⟨100⟩ direction. (b) $f = 0.40$, along the ⟨110⟩ direction. The experimental curve in (b) corrects the previously published Fig. 1(d) of Ref. [10], that has been reanalyzed and proved not valid due to sample contamination with air bubbles and oil.

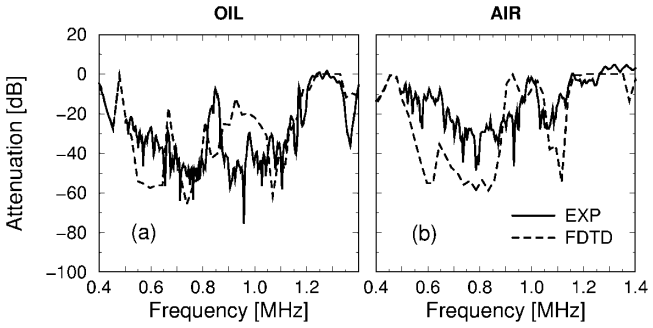

FIG. 4. Measured (solid lines) and calculated (dashed lines) attenuation vs frequency for two samples of Al with cylinders filled up with oil (a) and air (b). Parameters: $f = 0.4$, $\langle 100 \rangle$ direction.

sample with a 40% filling of oil, while in Fig. 4(b) the oil has been replaced by air. The measured attenuation for the oil slab is somewhat smaller than that of the samples filled with Hg, while the attenuation for the air sample is even weaker (although yet significant). Again here, the essential features of the experimental attenuation versus frequency curves (solid lines) are reproduced by the FDTD calculations (dashed lines). For both the Al-oil and the Al-air case other filling ratios and propagation over the $\langle 110 \rangle$ direction have been also measured and calculated, with the calculated results always in good agreement with the experimental data.

The calculations presented here solve the only physically meaningful equation for inhomogeneous systems including solids, that is, the full elastic wave equation. The transverse field component plays an essential role in the propagation that cannot be neglected applying the acoustic wave equation for these systems. The application of a FDTD scheme to integrate the acoustic equation ($\mu = 0$) leads, for the cases studied here, to results in full disagreement with the experimental observations [14]. The use of a FDTD scheme provides a reliable tool, necessary to explain recent experimental data on elastic band gap materials, that displays the propagation in time and space of ELW. Finally, elastic media provide a remarkable test system for many physical problems which now can also be investigated by the numerical resolution in real space and time of the full elastic wave equation. This work and the possibility of carrying out both experiments and calculations open up the way to new results in fields like localization due to disorder, interference, elastic wave guides, etc.

This work has been supported by Spanish DGICyT No. PB94-0151 and EU TMR No. ERBFMRXCT98-0242 projects. Ames Laboratory is operated for the U.S. Department of Energy by Iowa State University under Contract No. W-7405-Eng-82.

[1] C. Kittel, *Introduction to Solid State Physics* (Wiley, New York, 1971).
[2] E. Yablonovitch, Phys. Rev. Lett. **58**, 2059 (1987).
[3] S. John, Phys. Rev. Lett. **58**, 2486 (1987).
[4] K. M. Ho, C. T. Chan, and C. M. Soukoulis, Phys. Rev. Lett. **65**, 3152 (1990); K. M. Leung and Y. F. Liu, *ibid.* **65**, 2646 (1990); C. M. Soukoulis, *Photonic Band Gaps and Localization*, NATO ARW (Plenum, New York, 1993); M. M. Sigalas, E. N. Economou, and M. Kafesaki, Phys. Rev. B **50**, 3393 (1994).
[5] R. D. Meade, K. D. Brommer, A. M. Rappe, and J. D. Joannopoulos, Phys. Rev. B **44**, 13772 (1991); **44**, 10 961 (1991); E. Yablonovitch, T. J. Gmitter, R. D. Meade, A. M. Rappe, K. D. Brommer, and J. D. Joannopoulos, Phys. Rev. Lett. **67**, 3380 (1991); A. Mekis, J. C. Chen, I. Kurland, Shanhui Fan, Pierre R. Villeneuve, and J. D. Joannopoulos, Phys. Rev. Lett. **77**, 3787 (1996).
[6] M. M. Sigalas and E. N. Economou, Solid State Commun. **86**, 141 (1993); Europhys. Lett. **36**, 241 (1996); E. N. Economou and M. M. Sigalas, Phys. Rev. B **48**, 13 434 (1993); M. M. Sigalas, J. Appl. Phys. **84**, 3026 (1998).
[7] M. S. Kushwaha, P. Halevi, L. Dobrzynski, and B. Djafari-Rouhani, Phys. Rev. Lett. **71**, 2022 (1993); M. S. Kushwaha, P. Halevi, G. Martínez, L. Dobrzynski, and B. Djafari-Rouhani, Phys. Rev. B **49**, 2313 (1994).
[8] M. M. Sigalas and E. N. Economou, J. Sound Vib. **158**, 377 (1992).
[9] J. D. Achenbach and M. Kitahara, J. Acoust. Soc. Am. **80**, 1209 (1986); **81**, 595 (1987).
[10] F. R. Montero de Espinosa, E. Jiménez, and M. Torres, Phys. Rev. Lett. **80**, 1208 (1998).
[11] M. Torres, F. R. Montero de Espinosa, D. García-Pablos, and N. García, Phys. Rev. Lett. **82**, 3054 (1999).
[12] A. Taflove, *The Finite-Difference Time-Domain Method* (Boston, Artech House, 1998).
[13] L. D. Landau and E. M. Lifshitz, *Theory of Elasticity* (Pergamon, London, 1959).
[14] M. M. Sigalas, M. Kafesaki, and N. García (to be published).
[15] R. Clayton and B. Enquist, Bull. Seismol. Soc. Am. **67**, 1529 (1977).